Proceedings of the 28th International Conference on Ocean, Offshore and Arctic Engineering
OMAE2009
May 31 - June 5 , 2009, Honolulu, Hawaii

OMAE2009-80149

MODELING NONLINEAR IRREGULAR WAVES IN RELIABILITY STUDIES FOR OFFSHORE WIND TURBINES

P. Agarwal*
Stress Engineering Services
Houston, TX 77041, USA
Email: puneet.agarwal@stress.com

L. Manuel†
Dept. of Civil, Arch., and Env. Engineering
University of Texas
Austin, TX 78712, USA
Email: lmanuel@mail.utexas.edu

ABSTRACT

While addressing different load cases according to the IEC guidelines for offshore wind turbines, designers are required to estimate long-term extreme and fatigue loads; this is usually done by carrying out time-domain stochastic turbine response simulations. This involves simulation of the stochastic inflow wind field on the rotor plane, of irregular (random) waves on the support structure, and of the turbine response. Obtaining realistic response of the turbine depends, among other factors, on appropriate modeling of the incident wind and waves. The current practice for modeling waves on offshore wind turbines is limited to the representation of linear irregular waves. While such models are appropriate for deep waters, they are not accurate representations of waves in shallow waters where offshore wind turbines are most commonly sited. In shallow waters, waves are generally nonlinear in nature. It is, therefore, of interest to assess the influence of alternative wave models on the behavior of wind turbines (e.g., on the tower response) as well as on extrapolated long-term turbine loads. The expectation is that nonlinear (second-order) irregular waves can better describe waves in shallow waters. In this study, we investigate differences in turbine response statistics and in long-term load predictions that arise from the use of alternative wave models.

We compute loads on the monopile support structure of a 5MW offshore wind turbine model for several representative environmental states where we focus on differences in estimates of the extreme tower bending moment at the mudline due to linear and nonlinear waves. Finally, we compare long-term load predictions using inverse reliability procedures with both the linear and nonlinear wave models. We present convergence criteria that may be used to establish accurate 20-year loads and discuss comparative influences of wind versus waves in long-term load prediction.

INTRODUCTION

The calculation of long-term extreme loads is required in the design of offshore wind turbines according to the draft standard [1] from the International Electrotechnical Commission (IEC); this is usually done by carrying out stochastic turbine response simulations in the time domain. A flow chart outlining this procedure is presented in Fig. 1. First, the stochastic inflow wind field on the rotor plane and the irregular (random) waves on the support structure are simulated. The response, such as the bending moment at the base of the tower, to incident wind and waves is then computed in the time domain using an aeroelastic model of the turbine. One can then establish the distribution of load extremes using multiple simulations for each wind and wave combination; such conditional distributions are referred to as short-term distributions. Long-term loads, associated with a desired return period (on the order of 20-50 years, typically), can then be estimated using statistical extrapolation techniques. Clearly, the accuracy of predicted long-term loads depends, among other factors, on appropriate modeling of the incident wind and waves. The current practice to model waves on offshore wind turbines is limited to the use of linear irregular waves; this is not an accurate representation of waves in shallow waters where offshore wind turbines are most commonly sited. In shallow waters, waves are generally nonlinear in nature. It is, therefore, of interest to assess the influence of a nonlinear irregular wave model, such as the one proposed by Sharma and Dean [2], on extrapolated long-term turbine loads. In this study, we investigate differences in long-term turbine load predictions that arise from the use of linear versus nonlinear irregular wave models.

*Formerly, Graduate Research Assistant, University of Texas
†Corresponding Author

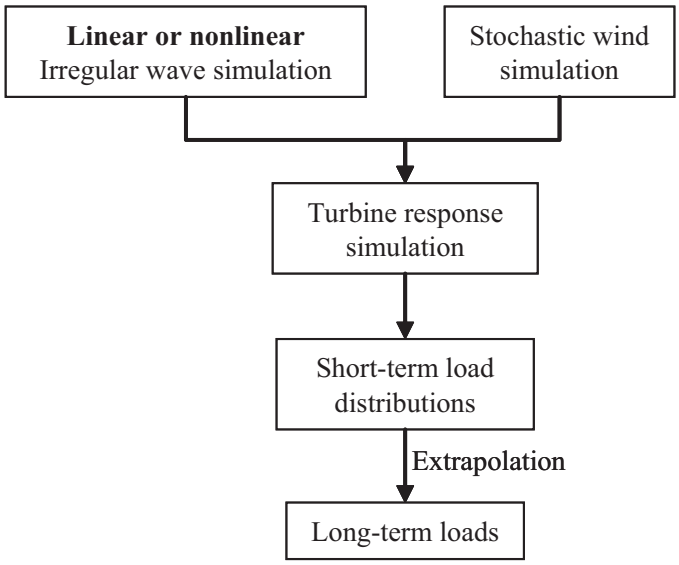

Figure 1. Flow chart outlining steps involved in estimating long-term turbine loads based on simulations.

Statistical extrapolation, the recommended method [1] to predict long-term loads for wind turbines, refers to estimation of a rare load fractile associated with a specified target long return period. Several extrapolation techniques, such as direct integration of short-term load distributions, conditional on environmental conditions, and appropriately weighted by the likelihood of occurrence of those conditions, as well as more efficient techniques such as the inverse first-order reliability method (inverse FORM) have been explored in wind turbine applications [3]. While extrapolated load estimates are known to be affected by statistical uncertainty, model uncertainty due to imperfect or unrealistic simulation models used can also result in errors in long-term load predictions. In a previous study [4], we focussed on how the sea surface elevation process, the water particle kinematics and, in particular, the derived hydrodynamic loads vary when nonlinear second-order waves are modeled as an alternative to the use of a conventional linear first-order approach. In the present study, we will specifically address the influence of model uncertainty, as it pertains to modeling of waves, on long-term turbine loads.

We use a utility-scale 5MW offshore wind turbine model developed at the National Renewable Energy Laboratory (NREL) [5] in our simulation studies. The turbine is assumed to be sited in 20 meters of water. Stochastic time-domain simulations of the turbine response are performed using the computer program, FAST [6]. We first present theoretical models for linear and nonlinear (second-order) irregular waves. For a coupled hydrodynamic and aeroelastic analysis of offshore wind turbines, we incorporate the nonlinear wave model in the computer program, FAST, for turbine simulations. We briefly discuss the procedure for long-term load extrapolation using the inverse FORM technique. We then compare the long-term loads based on linear and irregular wave models. We discuss short-term distributions of turbine loads for governing environmental states, and highlight the influence of nonlinear waves on these loads. An important question regarding the accuracy of extrapolation is related to the number of simulations required for each environmental state. Recently, we have shown that it is possible to systematically arrive at an appropriate number of simulations that must be carried out to satisfy specified convergence criteria [7]; we demonstrate application of this procedure here. Finally, we examine closely how the use of a nonlinear wave model affects turbine loads, particularly with larger wave heights, by focussing on large load occurrences in the response time series. From this, some insights are drawn on the importance of nonlinear waves on long-term extreme load prediction.

LINEAR AND NONLINEAR IRREGULAR WAVE MODELS

We are interested in computing hydrodynamic forces per unit length, $f(x,z,t)$, at any node located at a depth z (below the mean sea level), and along the centerline of a monopile (support structure for the turbine), which we arbitrarily define such that the horizontal coordinate x is set to zero; for simplicity of notation, we will denote $f(x,z,t)$ as f. We use Morison's equation [8] to compute the hydrodynamic forces, f, as follows:

$$f = f_D + f_M = \frac{1}{2} C_D \rho D (u - u_{str}) |u - u_{str}| + \left[C_M \frac{\pi D^2}{4} \rho \dot{u} - (C_M - 1) \frac{\pi D^2}{4} \rho \dot{u}_{str} \right] \quad (1)$$

where f_D and f_M are the drag and inertia forces per unit length, respectively. The drag coefficient, C_D, is taken to be 1.0, and the inertia coefficient, C_M, is taken to be 2.0 [5]. Variables, u and $\dot{u}$, represent the undisturbed water particle velocity and acceleration, respectively, at the point (x,z) of interest. Variables, u_{str} and $\dot{u}_{str}$, denote the velocity and acceleration at that same point, ρ is the density of water, and D is the monopile diameter. The horizontal water particle velocity, $u(x,z,t)$, and the horizontal water particle acceleration $\dot{u}(x,z,t)$ may be obtained from the velocity potential, $\Phi(x,z,t)$, by taking derivatives such that

$$u(x,z,t) = \partial \Phi(x,z,t)/\partial x; \quad \dot{u}(x,z,t) = \partial u(x,z,t)/\partial t. \quad (2)$$

Again, for simplicity, we will denote $\Phi(x,z,t)$ as Φ. According to the nonlinear irregular wave model of Sharma and Dean [2] and recommended in some guidelines for offshore structures [9], the velocity potential, Φ, may be thought to be comprised of first- and second-order components such that $\Phi = \Phi_1 + \Phi_2$. The first-order velocity potential is given as follows:

$$\Phi_1 = \sum_{m=1}^{N} b_m \frac{\cosh(k_m(h+z))}{\cosh(k_m h)} \sin \psi_m \quad (3)$$

where $b_m = A_m g/\omega_m$ and $\psi_m = (\omega_m t - \phi_m)$. Also, ω_m is the frequency of the m^{th} wave component and ϕ_m is the associated

random phase which is assumed to be uniformly distributed over $[0, 2\pi]$. The amplitudes of the individual wave components, A_m, are Rayleigh distributed random variables whose mean square value is given as $E[A_m^2] = 2S(\omega_m)d\omega$ where $S(\omega_m)$ refers to the one-sided power spectral density function of the sea surface elevation process. The integer, m, in Eq. 3 refers to a frequency index that ranges from 1 to N, the total number of wave components represented in the simulated wave train. Also, the linear dispersion relation, $\omega_m^2 = gk_m \tanh(k_m h)$, relates the wave number, k_m, to the frequency, ω_m, where h is the water depth and g is acceleration due to gravity.

The second-order velocity potential is given as follows:

$$\Phi_2 = \frac{1}{4}\sum_{m=1}^{N}\sum_{n=1}^{N}\left[b_m b_n \frac{\cosh(k_{mn}^{\pm}(h+z))}{\cosh(k_{mn}^{\pm}h)}\frac{D_{mn}^{\pm}}{(\omega_m \pm \omega_n)}\sin(\psi_m \pm \psi_n)\right] \tag{4}$$

where $k_{mn}^{\pm} = |k_m \pm k_n|$. Expressions for the transfer functions, $D_{mn}^{\pm}$, appearing in Eq. 4, are based on solution of Laplace's equation for the velocity potential with nonlinear boundary conditions given by Sharma and Dean [2]; these are also summarized by Agarwal and Manuel [10]. They (i.e., $D_{mn}^{\pm}$) are functions of frequency and wave number and are independent of the spectrum used. Second-order wave kinematics are thus obtained as a result of sum and difference interactions between pairs of frequencies. The phases of the second-order contributions as seen in Eq. 4 are also determined by sum and difference interactions of the phases of the first-order components, which are random.

Simulation of irregular (random) linear or first-order waves, which involves a single summation (Eq. 3), can be efficiently performed using the Inverse Fast Fourier Transform (IFFT). On the other hand, simulation of random nonlinear (second-order) waves, according to Eq. 4, involves a double summation which can be more expensive. However, one can rewrite this as a single summation by appropriately re-assembling and redefining indices (or coefficients) in the original double summation. Once the indices for an equivalent single summation are assembled, a one-dimensional IFFT procedure, similar to that for linear waves, can be used to perform the nonlinear wave simulations more efficiently. The nonlinear irregular wave model formulation discussed above has been incorporated into the computer program FAST [6], which performs coupled aeroelastic and hydrodynamic analysis of offshore wind turbines.

LOAD EXTRAPOLATION USING INVERSE FORM

Design Load Case 1.1b of the IEC 61400-3 draft design guidelines for offshore wind turbines [1] recommends the use of statistical extrapolation to predict rare extreme turbine loads. Direct integration and the inverse first-order reliability method (inverse FORM) [11] are two common extrapolation methods. For the same offshore wind turbine considered here, we have shown in an earlier study [12] that inverse FORM is as accurate as the direct integration method for predicting rare long-term load extremes. We only employ the inverse FORM procedure in the present study; however, for completeness of discussion, we briefly present the direct integration method.

In direct integration, one estimates the turbine characteristic load for design, l_T, associated with an acceptable probability of exceedance, P_T, or, equivalently, with a target return period of T years, as follows:

$$P_T = P[L > l_T] = \int_{\boldsymbol{X}} P[L > l_T | \boldsymbol{X} = \boldsymbol{x}]\, f_{\boldsymbol{X}}(\boldsymbol{x}) d\boldsymbol{x} \tag{5}$$

where $f_{\boldsymbol{X}}(\boldsymbol{x})$ represents the joint probability density function of the environmental random variables, $\boldsymbol{X}$, and L represents the load measure of interest. For different trial values of the load, l_T, Eq. 5 enables one to compute the long-term probability by integrating the short-term load exceedance probability conditional on $\boldsymbol{X}$, i.e., $P[L > l_T | \boldsymbol{X} = \boldsymbol{x}]$, with the relative likelihood of different values of $\boldsymbol{X}$. This method, while exact, is expensive as one is required to integrate over the entire domain of all the environmental random variables comprising $\boldsymbol{X}$. In the present study, two environmental random variables comprise $\boldsymbol{X}$; these are the ten-minute average wind speed, V, at hub height in the along-wind direction and the significant wave height, H_s, for waves assumed to be aligned with the wind.

In the Inverse FORM procedure, for the present application, one considers a surface in a three-dimensional space, $\boldsymbol{Y} = (V, H_s, L)$, of physical random variables, on one side of which (i.e., the "failure" side), it is assumed that $L > l_T$. It is possible to mathematically transform this space to an independent standard normal space $\boldsymbol{U} = (U_1, U_2, U_3)$. A sphere of radius, β, in this independent standard normal space can be constructed as follows:

$$u_1^2 + u_2^2 + u_3^2 = \beta^2 \tag{6}$$

This sphere is such that all values of $\boldsymbol{U}$ within it occur with a probability greater than $\Phi(-\beta)$ while all values outside it occur with a probability less than $\Phi(-\beta)$, where $\Phi()$ represents the cumulative distribution function of a standard normal random variable. It is noted here that β can be selected to be directly related to the target probability of load exceedance; namely, $P_T = \Phi(-\beta)$. The transformation of the relevant random variables from the physical $\boldsymbol{Y}$ space to the standard normal $\boldsymbol{U}$ space is carried out via the Rosenblatt transformation such that $F_V(v) = \Phi(u_1)$, $F_{H|V}(h) = \Phi(u_2)$, and $F_{L|V,H}(l) = \Phi(u_3)$, where $F()$ denotes a cumulative distribution function in each case. A point on the sphere defined by Eq. 6 where the load, L, attains its maximum value is the "design" point, and this load represents the desired characteristic T-year return period load, l_T.

According to the Inverse FORM procedure, we need to determine the appropriate load fractile level, $p_3 = \Phi(u_3)$, for all possible (V, H_s) pairs, with the constraint that the triad of associated values (u_1, u_2, u_3) must lie on the sphere of radius, β. The largest load upon consideration of all such values of u_3 and thus of p_3 yields the characteristic load, l_T. Based on Eq. 6, the fractile level, p_3, corresponding to the target reliability index, β, is obtained for each wind speed and wave height combination

(i.e., $(V, H_s) = (h, v)$) as follows:

$$p_3 = \Phi\left(\sqrt{\beta^2 - [\Phi^{-1}(F_V(v))]^2 - \left[\Phi^{-1}\left(F_{H|V}(h|v)\right)\right]^2}\right) \quad (7)$$

Extrapolation for the ultimate limit state requires data on load extremes, which must be obtained from turbine simulations. Any limitations or approximations inherent in a simulation model can influence the accuracy of long-term load predictions. One such model approximation in simulations is introduced by the conventional use of a linear theory to model waves. In this study, we focus on the influence on extrapolated long-term loads of linear versus nonlinear irregular wave modeling.

TURBINE MODEL

A 5MW wind turbine model developed at NREL [5] closely representing utility-scale offshore wind turbines being manufactured today is considered here. The turbine is a variable-speed, collective pitch-controlled machine with a maximum rotor speed of 12.1 rpm; its rated wind speed is 11.5 m/s. It is assumed to have a hub height that is 90 meters above the mean sea level, and a rotor diameter of 126 meters. It is assumed to be sited in 20 meters of water; it has a monopile support structure of 6 m diameter, which is assumed to be rigidly connected to the seafloor. The turbine is assumed to be installed at an IEC Class I-B wind regime site [1]. Kaimal power spectra and exponential coherence functions are employed to describe the inflow turbulence random field over the rotor plane, which is simulated using the computer program, TurbSim [13].

For the hydrodynamic loading on the support structure, irregular long-crested waves are simulated using a JONSWAP spectrum [14]. This same wave spectrum is used for simulating linear and nonlinear irregular waves. Hydrodynamic loads are computed using Morison's equation (Eq. 1); Wheeler stretching [9] is used to describe water particle kinematics and hydrodynamic loads up to the changing instantaneous sea surface.

Once time series of the full three-dimensional wind inflow turbulence field and the sea surface elevation are generated, stochastic time-domain simulations of the turbine response are carried out using the computer program, FAST [6]. FAST employs a combined modal and multi-body dynamics formulation for analysis of any turbine model. It models the tower and blades as flexible bodies and, in each case, uses the first two bending modes in the longitudinal and transverse directions. Additional details related to the modeling capabilities of FAST may be found in the User's Guide [6].

LONG-TERM TURBINE LOADS

Our interest is in predicting extreme loads for the selected offshore wind turbine (specifically, the fore-aft tower bending moment at the mudline) associated with a rare probability of exceedance level, corresponding to a return period of 20 years. To this end, we perform multiple simulations of the turbine response for various possible (V, H_s) combinations, followed by estimation of the fractile, p_3 (Eq. 7), of load extremes from short-term distributions of the load conditional on the environment. The maximum value of the different p_3 fractiles over all the environmental states yields the desired long-term load. In this study, we do not focus on the mechanics of the turbine response and the short-term distribution of extreme loads; these are discussed in detail elsewhere ([12] and [4]) for both linear and nonlinear wave models.

Table 1. Largest observed ten-minute maximum fore-aft tower bending moment at the mudline, from 500 simulations, for the governing environmental state for the linear wave model (V = 16 m/s, H_s = 5.5 m) and for the nonlinear wave model (V = 18 m/s, H_s = 7.5 m).

		Ten-minute maximum fore-aft tower bending moment at mudline		
V	H_s	wave model		
(m/s)	(m)	Linear (MN-m)	Nonlinear (MN-m)	ratio -
16	5.5	116.5	117.8	1.01
18	7.5	120.9	140.1	1.16

Calculations based on the use of the Inverse FORM procedure show that a mean wind speed, V, of 18 m/s and a significant wave height, H_s, of 7.5 m govern the long-term 20-year load when the nonlinear wave model is used. This is different from the governing values for V of 16 m/s and for H_s of 5.5 m when a linear wave model is used; this has been discussed in detail in a previous study by the authors [12]. Before presenting the actual long-term 20-year loads, we first compare these two environmental states.

Short-term Distributions

Ten-minute maximum fore-aft tower bending moments for two different critical environmental states based on 500 simulations are presented in Table 1. We used 500 simulations since the desired exceedance probability (1-p_3) for V = 18 m/s and H_s = 7.5 m is 2.03×10^{-3}, which could be empirically estimated to within less than an order of magnitude with that number of simulations. For comparison, we also carried out 500 simulations for V = 16 m/s and H_s = 5.5 m, although this environmental state requires a rarer (3.87×10^{-6}) probability of exceedance of load given environment. Table 1 shows that the observed maximum load from 500 simulations is almost the same with linear and nonlinear wave models for V = 16 m/s and H_s = 5.5 m; this was discussed in detail in an earlier study [4]. For V = 18 m/s and H_s = 7.5 m, on the other hand, observed maximum loads increase significantly—by about 16%—when the wave model is changed from linear to nonlinear. This is again in line with findings in our earlier study [4], where we showed that for larger significant wave heights, use of a nonlinear wave model results in a significant increase in hydrodynamic loads.

Figure 2 shows empirical (short-term) probability distributions of ten-minute load (fore-aft tower bending moment at the mudline) maxima when linear and nonlinear waves are used for

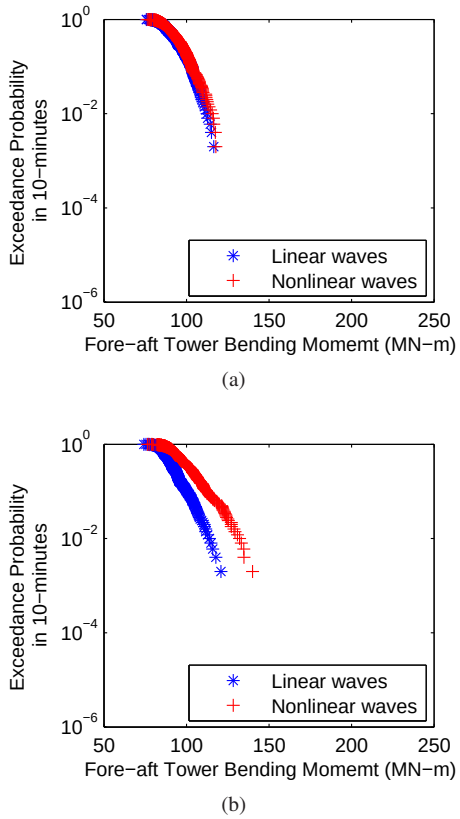

Figure 2. Empirical probability distributions of ten-minute maxima of the fore-aft tower bending moment at the mudline based on 500 ten-minute simulations for (a) V = 16 m/s, H_s = 5.5 m; and (b) V = 18 m/s and H_s = 7.5 m.

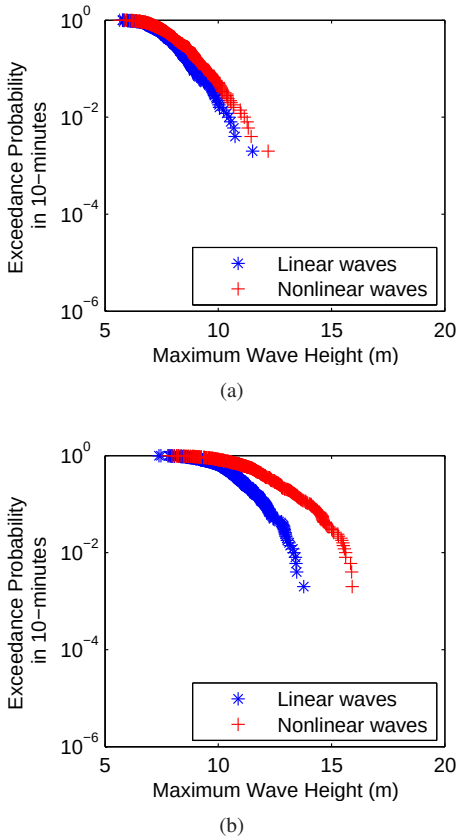

Figure 3. Empirical probability distributions of ten-minute maxima of the wave height based on 500 ten-minute simulations for (a) V = 16 m/s, H_s = 5.5 m; and (b) V = 18 m/s and H_s = 7.5 m.

the two selected environmental states. The distributions of load maxima with linear and nonlinear waves are quite different for V = 18 m/s and H_s = 7.5 m, while they are almost identical for V = 16 m/s and H_s = 5.5 m. It is interesting to note that these trends are similar for short-term distributions of ten-minute maximum wave heights (crest to trough), which are shown in Fig. 3. This is because hydrodynamic loads on this monopile (of 6 m diameter) are governed by inertia forces (see Agarwal and Manuel [10, 4] for details), which are directly proportional to wave height. It is worth noting that differences in probability distributions for loads resulting from using linear and nonlinear wave models are not as pronounced as they are for wave heights. This is because loads on this wind turbine are primarily driven by wind; waves are only of secondary importance.

Convergence Check for Rare Load Fractiles

While we have performed 500 ten-minute simulations, resulting in 500 load extremes, for these two environmental states, in practice, a much smaller number of simulations is typically carried out for extrapolation. With a small number of simulations, however, the accuracy of tails of any short-term distribution and of estimates of rare fractiles becomes questionable. In an earlier study [7], we proposed use of convergence criteria, which compared confidence bounds (e.g., at the 90% level) on an observed rare percentile (e.g., the 84$^{\text{th}}$ percentile) of the short-term load distribution versus an imposed acceptable limit, to establish how many simulations would be adequate in order to have a stable distribution especially in the tails. Table 2 shows estimates of the 84$^{\text{th}}$ percentile 10-minute maximum load from ten separate sets of 50 simulations each. The average of the ten estimates, shown in Table 2, is very close to the estimate of the 84$^{\text{th}}$ percentile load from 500 simulations, which is 100.0 MN-m (with linear waves) and 100.7 MN-m (with nonlinear waves) for V = 16 m/s, H_s = 5.5 m; and 96.1 MN-m (with linear waves) and 108.3 MN-m (with nonlinear waves) for V = 18 m/s, H_s = 7.5 m. This suggests that 50 simulations may be sufficient to yield a stable estimate of a rare load fractile. It can also be seen that the 84$^{\text{th}}$ percentile load estimate for all the cases is very stable, and it has a range (as defined in Table 2) that is always less than 10%. This range on the 84$^{\text{th}}$ percentile loads, which is essentially the 82% (10/11 - 1/11 = 9/11 = 0.82) confidence interval, normalized relative to the median estimate, is larger for nonlinear waves for both the environmental states. This is expected since nonlinear waves are more non-Gaussian and result in larger variability in turbine loads as well.

The 90% confidence bounds on the 84$^{\text{th}}$ percentile load, obtained using bootstrap techniques [15], are summarized in Table 3. These so-called relative confidence bounds (which are normalized relative to the point estimate of the 84$^{\text{th}}$ percentile load average from 10 sets of 50 simulations), are less than 10% for both environmental states, with either linear or nonlinear waves. In an earlier study [7], we suggested that a given number of sim-

Table 2. Estimates of the 84th percentile 10-min maximum fore-aft tower bending moment at the mudline from 10 separate sets of 50 simulations each.

	84th percentile 10-min maximum fore-aft tower bending moment from 50 simulations (in MN-m)			
	V = 16 m/s, H_s = 5.5 m		V = 18 m/s, H_s = 7.5 m	
Waves: Set No.	linear	nonlinear	linear	nonlinear
1	100.1	100.0	97.6	108.2
2	98.6	99.6	97.8	108.4
3	101.2	101.5	98.8	113.3
4	97.8	100.2	98.4	106.0
5	104.8	107.3	96.4	110.2
6	98.8	98.8	93.2	107.0
7	100.0	100.2	94.4	106.4
8	98.6	100.4	96.1	108.2
9	99.5	100.5	94.9	106.8
10	98.9	100.2	96.7	111.8
Average	99.8	101.0	96.4	108.6
Range	7.0%	8.4%	5.7%	6.7%

Note: Range = 100×(Max - Min)/Median, over 10 sets

ulations is adequate for obtaining a stable short-term distribution if its relative confidence bound is confirmed to be less than 15%, which is the case here. Moreover, we see in Table 3, that the relative confidence bounds decrease significantly when all 500 simulations are used in a similar bootstrapping exercise. Besides, the 90% relative confidence bounds presented in Table 3, which are estimated using bootstrap resamplings, are all smaller than the 82% confidence bounds shown in Table 2, which were estimated from non-repeating sets of real data (albeit only from ten sets). This is also expected as bootstrap resamplings (with replacement) give smaller confidence bounds than real non-repeating random samples [16]. In summary, the stable estimates of a rare fractile and associated acceptable confidence bounds seen here suggest that 50 simulations are adequate for extrapolation. We now discuss extrapolated 20-year tower loads for the selected offshore wind turbine.

Table 3. Estimates of the 90% relative confidence bound (RCB) on the 84th percentile 10-min maximum fore-aft tower bending moment at the mudline.

	90% RCB on 84th percentile 10-min maximum fore-aft tower bending moment (in %)			
	V = 16 m/s, H_s = 5.5 m		V = 18 m/s, H_s = 7.5 m	
Waves: # sims.	linear	nonlinear	linear	nonlinear
50	6.9	6.1	7.8	8.6
500	2.3	1.8	2.6	3.1

Table 4. Extrapolated 20-year loads based on 50 10-min simulations.

	Extrapolated 10-min maximum fore-aft tower bending moment (in MN-m)					
	V = 16 m/s, H_s = 5.5 m			V = 18 m/s, H_s = 7.5 m		
	lin.	nonlin.	ratio	lin.	nonlin.	ratio
Min	116.9	118.5	1.01	110.8	125.0	1.13
Max	132.9	137.8	1.04	121.2	142.4	1.17
Median	125.6	128.1	1.02	117.7	138.4	1.18
Max. obs.	116.5	117.8	1.01	120.9	140.1	1.16

Notes: Min, Max and Median are statistics of extrapolated loads over 10 sets. Max. obs. is the largest observed load from 500 simulations.

Extrapolated Loads

Table 4 summarizes extrapolated 20-year loads (resulting from estimates of p_3 fractiles—see Eq. 7)using Inverse FORM. Listed are the minimum, maximum, and median estimates of these 20-year loads obtained from ten sets of 50 simulations. To estimate the p_3-load fractile, a two-parameter Weibull distribution was fitted to the above-median (i.e., the largest 25 load extremes out of 50) load extremes. The required target exceedance probabilities (= 1 - p_3) are 2.03×10^{-3} and 3.87×10^{-6} for V = 18 m/s, H_s = 7.5 m and V = 16 m/s, H_s = 5.5 m, respectively. It can be seen that the extrapolated loads are larger when nonlinear waves are modeled, with a difference of about 18% on the median for V = 18 m/s, H_s = 7.5 m. The normalized range of the predicted long-term loads (= 100×(Max - Min)/Median) is 15% or smaller for all cases. As was the case for the range on the 84th percentile loads summarized in Table 2, the computed range on 20-year loads in Table 4 is larger for nonlinear waves, indicating greater variability compared to with the use of linear waves. Also, it should be noted that the extrapolated 20-year loads are very close to the largest empirically observed load (from 500 simulations) for V = 18 m/s, H_s = 7.5 m; this is because the largest observed extreme from 500 simulations is associated with an exceedance probability of $1/501$ or 1.996×10^{-3}, which is close to the desired (1 - p_3) exceedance probability of 2.03×10^{-3}.

Relation between Large Wave Heights and Large Loads

To further understand how waves influence loads for the two environmental states studied, we investigate whether the occurrence of the maximum fore-aft tower bending moment in a ten-minute time series and the occurrence of the maximum instantaneous wave height in that same time series are close (i.e., well correlated) or far apart (i.e., less correlated) in time. Maximum wave heights and maximum loads that occur close to each other in time are possible indications that the large waves might be causing the large loads; such a case can be seen, for example, in Fig. 4. We select a time separation (to distinguish well correlated from less correlated maximum load-wave pairs) to be equal

to the peak spectral period of the waves. Scatter plots of well and less correlated events are presented in Figs. 5 and 6 for V = 16 m/s and H_s = 5.5 m and for V = 18 m/s and H_s = 7.5 m, respectively; the total number of events are indicated on each of the plots. Each event represents a single matching maximum wave height and load from a 10-min simulation. A total of 500 simulations are represented; hence, the sum of well correlated and less correlated events equals 500. It is seen that for V = 16 m/s and H_s = 5.5 m, the fraction of well correlated events is about 9% and 14% for linear and nonlinear waves, respectively. For V = 18 m/s and H_s = 7.5 m, the fraction of well correlated events is much higher—about 21% and 44% for linear and nonlinear waves, respectively. For both environmental conditions, the fraction of well correlated events is seen to be larger when nonlinear wave models are considered. For V = 18 m/s and H_s = 7.5 m, this fraction is almost doubled, which is consistent with our earlier observation that nonlinear waves for this environmental state result in larger wave heights and, consequently, larger loads. For V = 18 m/s and H_s = 7.5 m, it can also be seen from the scatter plots (Fig. 6) that simulated loads are significantly larger with nonlinear waves than with linear waves. Furthermore, the scatter plot shows strong positive correlation between maximum wave heights and maximum loads for the nonlinear wave model only for V = 18 m/ sand H_s = 7.5 m. This clearly indicates that nonlinear waves, especially for large wave heights, have a clear influence on loads; note that this is not the case for linear waves.

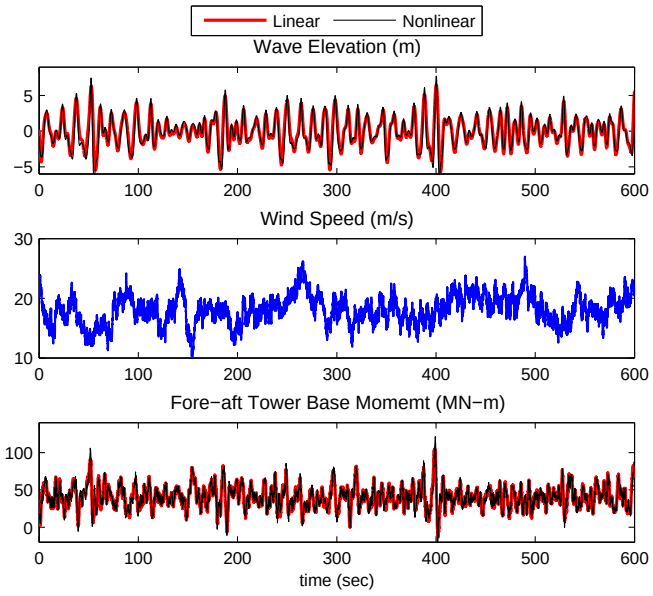

Figure 4. Ten-minute time series of the sea surface elevation, the hub-height longitudinal wind velocity, and the fore-aft tower base bending moment showing almost concurrent occurrences of the maximum wave height and the maximum tower load for V = 18 m/s, H_s = 7.5 m.

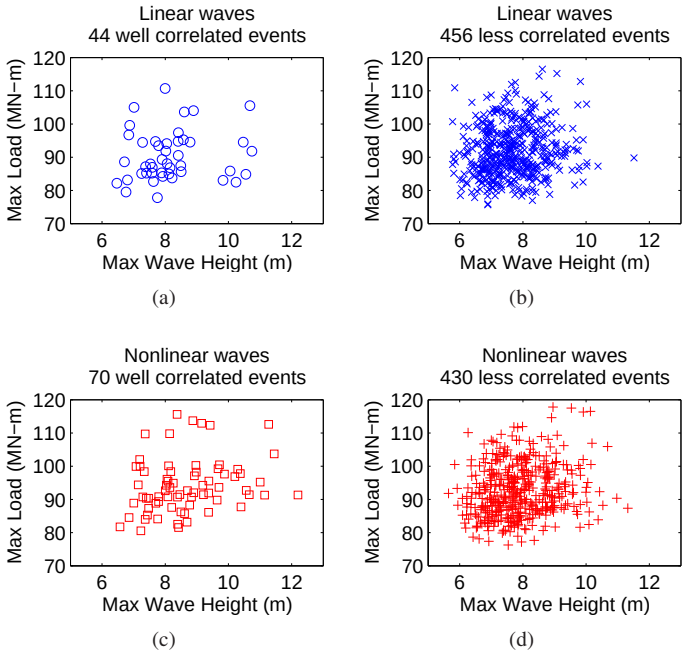

Figure 5. Scatter plots showing whether the occurrence of the maximum fore-aft tower bending moment in ten minutes and that of the maximum instantaneous wave height are close (i.e., well correlated) or far apart (i.e., less correlated). Plots are for V = 16 m/s and H_s = 5.5 m.

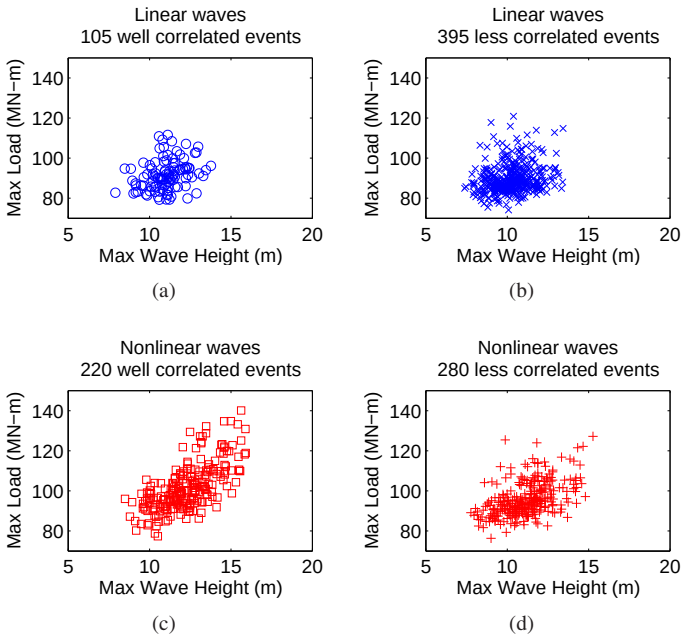

Figure 6. Scatter plots showing whether the occurrence of the maximum fore-aft tower bending moment in ten minutes and that of the maximum instantaneous wave height are close (i.e., well correlated) or far apart (i.e., less correlated). Plots are for V = 18 m/s and H_s = 7.5 m.

In summary, the governing environmental state for long-term loads for the selected offshore wind turbine changed from V = 16 m/s and H_s = 5.5 m when linear waves are modeled to V = 18 m/s and H_s = 7.5 m when nonlinear waves are modeled, and the 20-year load increased by about 10%. This is because at larger wave heights, wave loads, relative to wind loads, become more important when a nonlinear wave model is used. Therefore, in estimating long-term loads for an offshore wind turbine sited in shallow water depths, it is important that nonlinear irregular waves are modeled.

Summary and Conclusions

Our objective in this study was to investigate the effect of alternative irregular wave models on long-term loads for a utility-scale 5MW offshore wind turbine sited in 20 meters of water. Our focus was on the fore-aft tower bending moment at the mudline. We used a nonlinear (second-order) irregular wave model which, for shallow water depths, is more appropriate than the more commonly used linear irregular wave model. We incorporated this nonlinear wave model in a time-domain simulator that performs aero-servo-hydro-elastic analysis of offshore wind turbines. We studied the influence of linear and nonlinear wave models on extreme loads on a monopile support structure (a cylinder of 6 m diameter) of the turbine.

To compute long-term loads, we used the Inverse First-Order Reliability Method (FORM). We found that 20-year loads increased by about 10% when wave models were changed from linear to nonlinear. More importantly, the governing environmental state changed from V = 16 m/s and H_s = 5.5 m when linear waves were modeled to V = 18 m/s and H_s = 7.5 m when nonlinear waves were modeled. The relative contribution of waves to wind towards overall long-term loads increased at this latter environmental state. Besides, we showed that confidence intervals on rare load fractiles estimated from short-term distributions were within acceptable limits for the number of simulations carried out; this suggests a reasonable accuracy in long-term load predictions.

By studying correlations of the occurrences of the largest 10-min loads and the largest 10-min wave heights for the governing environmental state, we determined that the influence of the use of a nonlinear wave model becomes clearly more pronounced at larger wave heights. This suggests that modeling of nonlinear waves is especially important at sites where wave heights can be large.

In summary, this study suggests that nonlinear irregular waves have an important influence on the long-term loads on an offshore wind turbine support structure, even while the turbine is in operation when loads due to wind are generally much larger than those due to waves. Therefore, nonlinear irregular waves should be considered when predicting long-term loads for offshore wind turbine design.

ACKNOWLEDGMENT

The authors are pleased to acknowledge the financial support received from the National Science Foundation by way of two grants—Award Nos. CMMI-0049128 (CAREER) and CMMI-0727989. They also thank Dr. Jason Jonkman at the National Renewable Energy Laboratory for assistance with the wind turbine simulation model used in this study.

REFERENCES

[1] IEC-61400-3, 2005. *Wind Turbines - Part 3: Design Requirements for Offshore Wind Turbines*. International Electrotechnical Commission, TC88 WG3 Committee Draft.

[2] Sharma, J. N., and Dean, R. G., 1979. Development and Evaluation of a Procedure for Simulating a Random Directional Second-order Sea Surface and Associated Wave Forces. Tech. Rep. Ocean Engineering Report No. 20, University of Delaware, Newark, DE.

[3] Saranyasoontorn, K., and Manuel, L., 2006. "Design Loads for Wind Turbines using the Environmental Contour Method". *Journal of Solar Energy Engineering, Transactions of the ASME,* **128**(4), pp. 554–561.

[4] Agarwal, P., and Manuel, L., 2008. "On the Modeling of Nonlinear Waves for Prediction of Long-Term Offshore Wind Turbine Loads". In 27th International Conference on Offshore Mechanics and Arctic Engineering, OMAE 2008.

[5] Jonkman, J. M., Butterfield, S., Musial, W., and Scott, G., 2007 (to be published). Definition of a 5-MW Reference Wind Turbine for Offshore System Development. Tech. Rep. NREL/TP-500-38060, National Renewable Energy Laboratory, Golden, CO.

[6] Jonkman, J. M., and Buhl Jr., M. L., 2005. FAST User's Guide. Tech. Rep. NREL/EL-500-38230, National Renewable Energy Laboratory, Golden, CO.

[7] Fogle, J., Agarwal, P., and Manuel, L., 2008. "Towards an Improved Understanding of Statistical Extrapolation for Wind Turbine Extreme Loads". *Wind Energy - Special Issue on Design Load Definition,* **11**(6), pp. 613–635.

[8] Barltrop, N., and Adams, A., 1991. *Dynamics of Fixed Marine Structures*. Butterworth-Heinemann, London.

[9] DNV-RP-C205, 2007. *Environmental Conditions and Environmental Loads, Recommended Practice*. Det Norske Veritas.

[10] Agarwal, P., and Manuel, L., 2008. "Wave Models for Offshore Wind Turbines". In ASME Wind Energy Symposium, AIAA.

[11] Winterstein, S. R., Ude, T. C., Cornell, C. A., Bjerager, P., and Haver, S., 1993. "Environmental Contours for Extreme Response: Inverse FORM with Omission Factors". In Proceedings, ICOSSAR-93.

[12] Agarwal, P., and Manuel, L., 2007. "Simulation of Offshore Wind Turbine Response for Extreme Limit States". In 26th International Conference on Offshore Mechanics and Arctic Engineering, OMAE 2007.

[13] Jonkman, B. J., and Buhl Jr., M. L., 2007. TurbSim User's Guide. Tech. Rep. NREL/TP-500-41136, National Renewable Energy Laboratory, Golden, CO.

[14] DNV-OS-J101, 2007. *Design of Offshore Wind Turbine Structures, Offshore Standard*. Det Norske Veritas.

[15] Efron, B., and Tibshirani, R. J., 1993. *An Introduction to the Bootstrap*. Chapman and Hall, New York.

[16] Efron, B., and Tibshirani, R. J., 1991. "Statistical Data Analysis in the Computer Age". *Science,* **253**(5018), pp. 390–395.